



# Influence of shear connector type and degree on semi-rigid joints of composite cold-formed steel beam-to-column connections

Mustafa S. Salah<sup>1</sup> · Haitham H. Muteb<sup>2</sup>

Received: 3 November 2023 / Revised: 17 March 2024 / Accepted: 27 May 2024  
© The Author(s), under exclusive licence to Springer Nature Switzerland AG 2024

## Abstract

This paper presents findings from an experimental study focused on a composite connection between a composite concrete slab and two cold-formed steel C-sections. These sections are positioned in a back-to-back arrangement, serving as both a beam and a column. The study involved testing five specimens of cruciform subassemblies of cold-formed steel (CFS) beam-to-column joints with different shear connection types and degrees of the bolted shear connector. The results obtained from testing the specimens were presented, including their moment capacity, rotational capacity, the slip of the concrete slab, and modes of failure. All the specimens showed high ductile properties with a rotation capacity exceeding 30 mrad, indicating that they are semi-rigid joints that are suitable for plastic analysis and seismic design, according to Eurocode 4 (EC4). The novel approach used in the CFS angle plate shear connector significantly improved the moment and initial stiffness of the joint. The partially bolted shear connector used in the study produced satisfactory results and was within the recommended limits for semi-rigid joints according to the European Code. As a result, the study suggests that the current restrictions on providing full shear connection design within semi-continuous structure-hogging moment regions could be relaxed.

**Keywords** Composite joint · CFS · Beam-to-column onnection · Semi-rigid joint · Shear connector · Bolted shear connector

## 1 Introduction

Because of their numerous advantages, such as ease of fabrication and assembly, good seismic performance, and adequate fire resistance, beam-to-column composite bolted joints are widely used in building engineering [1–5]. A typical composite joint system comprises universal beams connected to columns via various connections such as endplates, seat cleat angles, assembly plates, etc. Shear connectors are typically used to connect a concrete slab to the top edge of a beam and play an essential role in joint behavior. Many studies focus on the composite connection between the steel beam and concrete slab. Fu, F., and Lam, D [6]. investigated

the semi-rigid beam-to-column connection with different stud spacing, spacing of the first shear connector from the face of the column, shear connector degree, the cross-section area of the longitudinal bar, and slab thickness experimentally. From the results, a full shear connection should be used to allow full mobilization of the longitudinal reinforcement. In contrast, a partial shear connection would reduce moment and rotation capacity because the longitudinal bars could not be fully mobilized. It also shows that the location of the headed studs had a significant impact on the rotation capacity of the composite connections.

Loh, H. Y. et al. [7] conducted an empirical examination of the impact of partial shear connection within composite flush end plate joints. For this investigation, they manufactured six specimens, each designed with varying quantities of shear connections and different reinforcement ratios. The findings revealed that decreasing the shear connection level led to achieving the peak moment at an increased rotational value. The utilization of partial shear connection demonstrated the advantages of heightened ductility while retaining stiffness and strength, offering valuable insights for plastic

✉ Mustafa S. Salah  
mustafa.sa@uowa.edu.iq

<sup>1</sup> Civil Engineering Department, College of Engineering, University of Warith Al-Anbiyaa, Karbala 56001, Iraq

<sup>2</sup> College of Engineering, University of Babylon, Babylon, Iraq

design in continuous and semi-continuous composite structures. Moreover, elevating the reinforcement levels might enhance moment and rotation capacities, but this effect only persists up to a certain threshold. Based on the test outcomes, the optimal range for reinforcement seems to fall between 1.0 and 1.5% of the effective slab area. Four full-scale specimens are prepared by Ataei A. et al. [8] to investigate the influence of bolted shear connector type, degree of shear connection, and type of precast concrete slab on the structural behavior of deconstructable composite joints. The test findings reveal that reduced shear connections lead to a reduction in the initial capacity of a composite joint, which can increase the deflection of the composite beams under service-load conditions. Furthermore, small bolted shear connectors give small slips at different load levels.

On the other hand, as long as cold-formed steel (CFS) has economic potential and produces a better design, the use of CFS in composite connections could be more popular and convincing than the hot-rolled profile. The CFS is a cutting-edge and dependable alternative to hot-rolled steel. Additionally, due to the impracticality of using the headed stud—a prevalent shear connector for hot-rolled steel beams—with cold-formed steel beams, there arises a need for further exploration into novel shear connectors suitable for cold-formed steel composite structures. Consequently, researchers have initiated the process of designing and evaluating different shear connectors tailored for components of cold-formed steel composites [9–15].

However, because the common shear connector for hot-rolled steel beams, the headed stud, is not suitable for cold-formed steel beams, more research into new shear connectors for cold-formed steel composite structures is required. As a result, researchers began developing and testing different shear connectors for cold-formed steel composite parts [16].

Some studies have addressed the effect of the angle shear connector because of its role in improving shear resistance and enhancing the bond between the steel beam and the concrete slab [17–19]. However, to the best of the authors' knowledge, the effect of using an angle or corrugated plate shear connector with cold-formed composite members and its effect on the performance of the beam-to-column joint has not been studied. Therefore, in this study, this type of connector was proposed.

But the use of these shear connectors with composite CFS section joints is still limited, and the use of CFS is still limited to low-rise buildings with a short span. So, this study aims to discuss the shear connection effect on the composite CFS beam-to-column joint. Five composite joint specimen tests were performed to investigate the behavior of various shear connectors, including a bolted shear connector with a single embedded nut and CFS plate shear connectors. The

performance and structural behavior of these connections are studied in this paper, including the effect on the composite joint's behavior, failure shape, ultimate moment, rotational capacity, initial stiffness, and strain distribution.

## 2 Experimentalwork

### 2.1 Specimen design and details

Five specimens with cruciform subassemblies of cold-formed steel beam-to-column joints were carried out in this study. All samples tested were identical in terms of steel beam section, column section, concrete slab thickness, and top and seat angle plate connection but different in degree and type of shear connector. Which carried out in a novel approach to different shear connections: single embedded nut bolt, cold-formed angle plate, and cold-formed corrugated plate, as shown in Fig. 1. The cold-formed steel used for the beam and column has a lipped double-channel section with a thickness of 3 mm and a depth of 150 and 200 mm, respectively. The beam and column were joined by an angle from the top and seat only and were made from CFS with an 8 mm thickness. The concrete slab had a thickness of 70 mm and a width of 750 mm and was reinforced by  $\varnothing 10 @ 100$  mm in both directions. The M20 bolts grade 8.8 were used as fasteners, where they were installed using the torque screwdriver. The details are depicted in Figs. 2 and 3 and summarized in Table 1.

Figure 4 illustrates the sequence of fabrication stages for the composite joint specimen. Initially, the cold-formed steel (CFS) beams and columns were manufactured using a hydraulic press brake machine. Subsequently, the flanges of the CFS sections were perforated using a drill machine. Lastly, a wooden mold was crafted and subsequently filled with normal strength concrete. The resulting concrete slabs underwent a curing period of 28 days. In Fig. 5, the nomenclature system assigned to each specimen is presented. The specimen is denoted by the letter 'CJ' followed by the shear connector type (e.g. T1 = bolted shear connector) and the degree of the bolted shear connector (e.g. D100 = specimen have a fully bolted shear connector with 16 bolt).

### 2.2 Material properties

The CFS plate, utilized to construct the beam, column, top and seat angles, as well as shear connectors, underwent a coupon test in accordance with ASTM (A370-05) [20]. Furthermore, standard 10 mm diameter bars, serving as both longitudinal and transverse reinforcement within the concrete slabs of the composite joint specimens, were also subjected to testing. The outcomes of these tests are presented

Fig. 1 Details of shear connector types

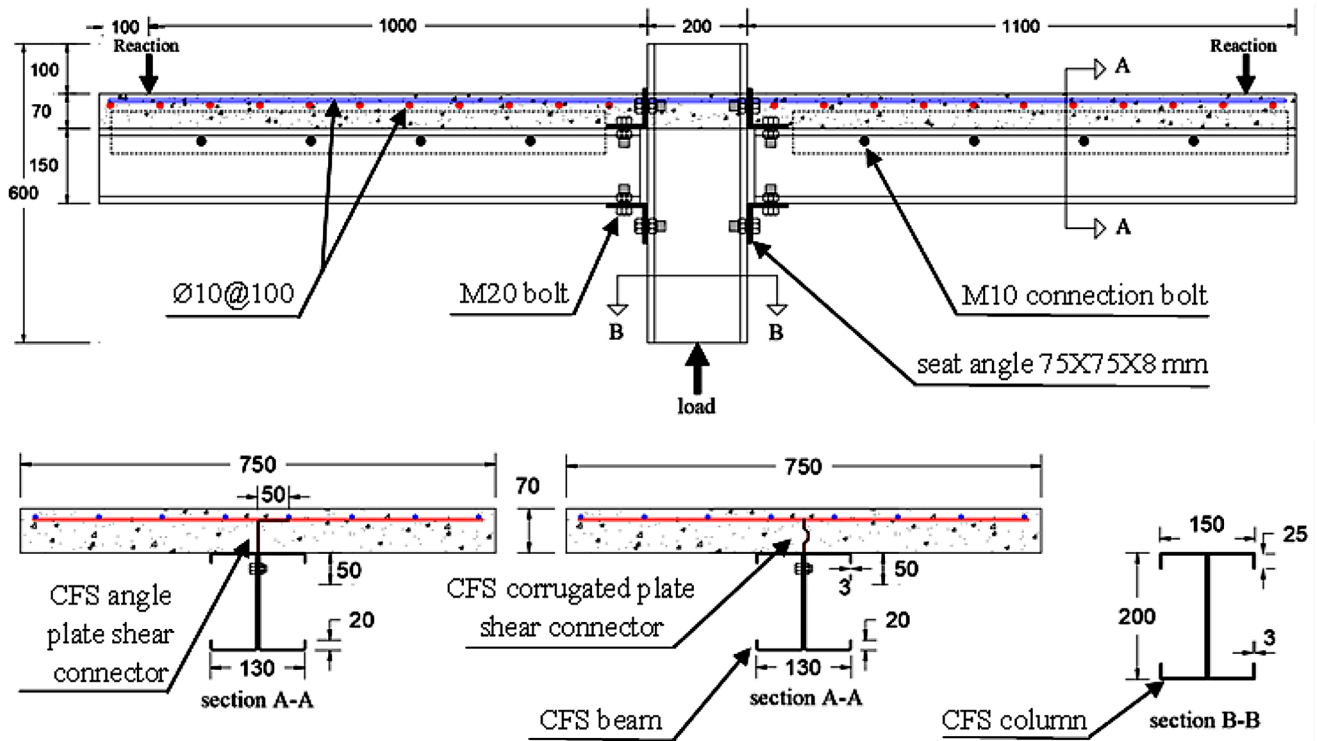
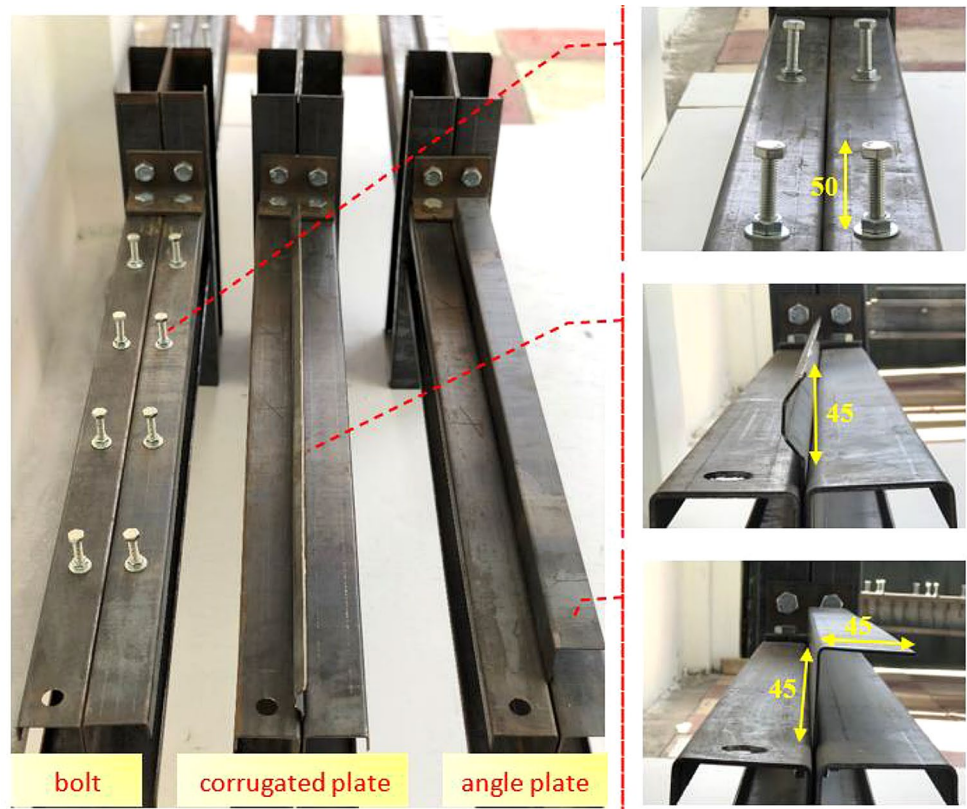


Fig. 2 Details of specimens CJT<sub>2</sub> and CJT<sub>3</sub>

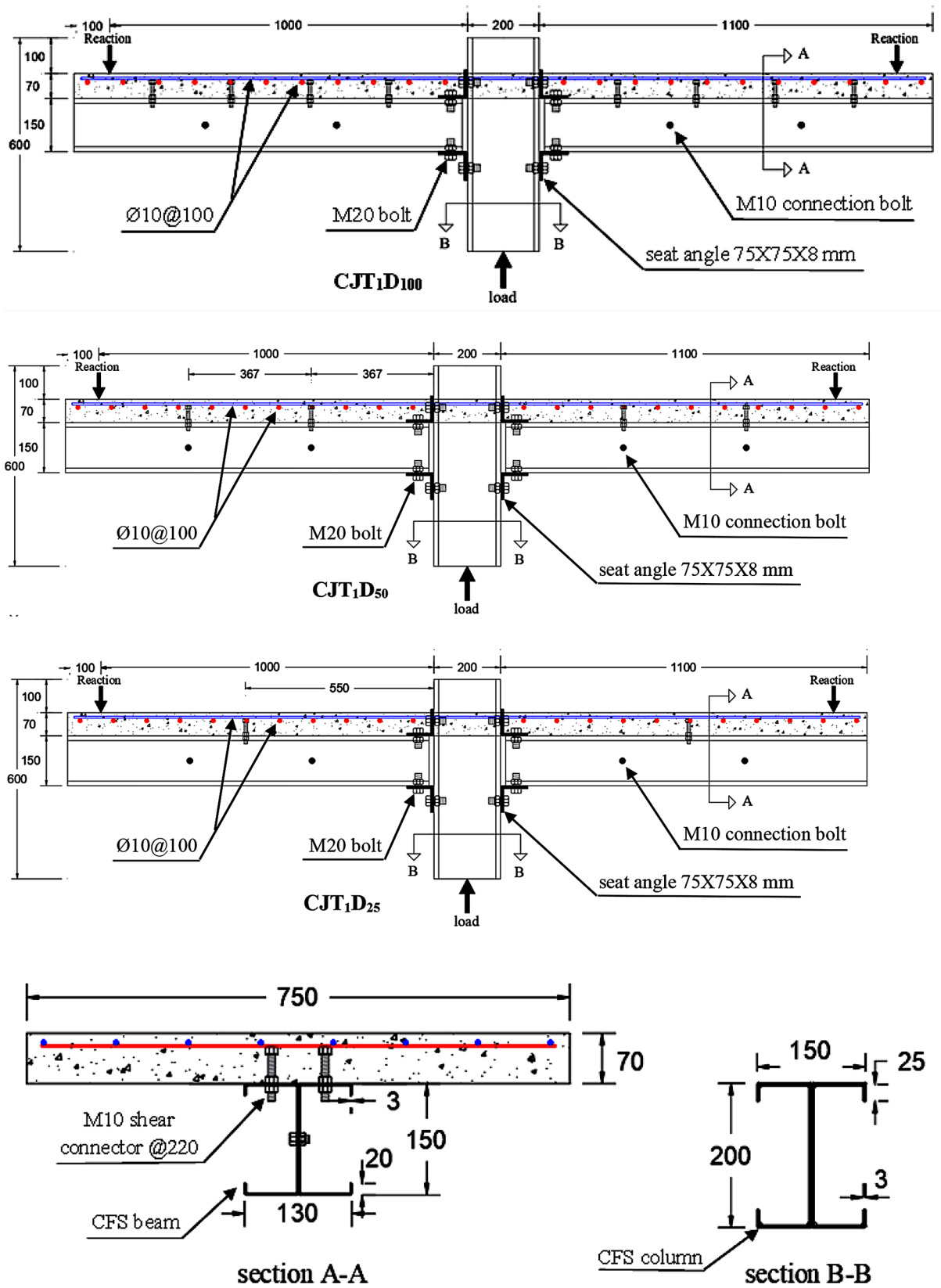


Fig. 3 Details of specimens with different bolted shear connector degrees



**Table 1** Composite joint specimens' details

Specimen	Shear connector type	Number of bolted shear connector
CJT <sub>1</sub> D <sub>100</sub>	single embedded nut bolt	16
CJT <sub>1</sub> D <sub>50</sub>	single embedded nut bolt	8
CJT <sub>1</sub> D <sub>25</sub>	single embedded nut bolt	4
CJT <sub>2</sub>	cold-formed angle plate	-
CJT <sub>3</sub>	cold-formed corrugated plate	-

in Table 2. Notably, the concrete's compressive strength was determined through 150 × 300 mm cylinder tests and found to be 30 MPa. Additionally, the concrete's tensile strength was evaluated from both splitting and flexural tests, resulting in values of 3.08 MPa and 3.90 MPa, respectively.

### 2.3 Instrumentation

Four linear variable displacement transducers (LVDT) were used in this study. The LVDT1 and LVDT2 are put at the bottom and top of the beam web to measure the joint's rotation. The deflection under the column and the slip between the slab and the steel beam were also measured by LVDT3 and LVDT4, respectively, as shown in Fig. 6. Because of the symmetrical loading, it was expected that the column rotation would be negligible and thus have no effect on the rotation of the connection. During the tests, this was confirmed.

**Fig. 4** Specimen preparation: **a** manufacturing CFS section, **b** perforate the CFS flange, **c** assembly of parts and **d** concrete casting and curing

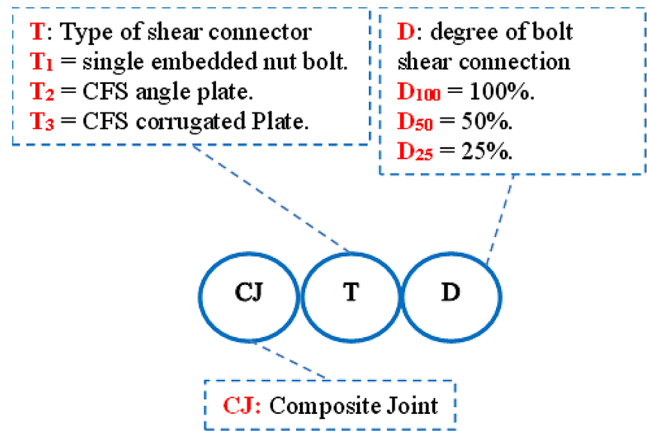
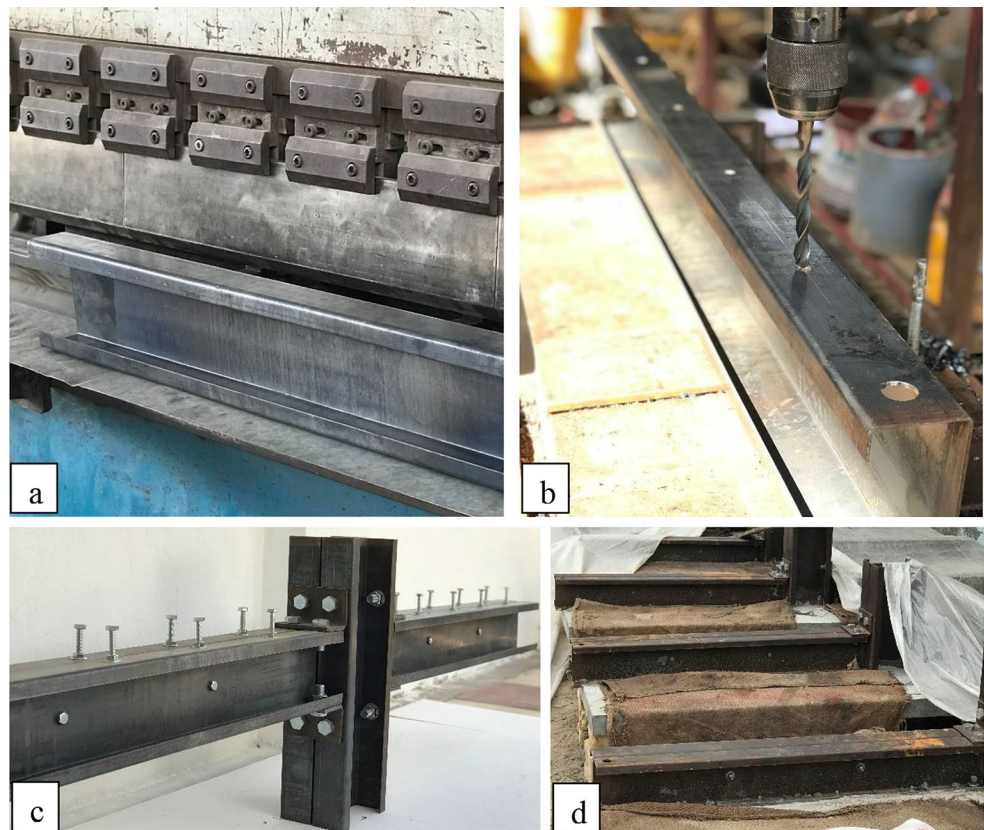


**Fig. 5** The composite joint specimen nomination system

Besides the LVDT measurements, a 2D digital image correlation (DIC) measurement system was used in tests of composite beam-to-column specimens due to its accuracy in capturing the deformation in structures, which is used to study a wide variety of material performances. The objective of the deformation analysis in the present study is to examine the linear strain, different deformation components in the joints of the beam-to-column connections, and the slip between the cold-formed steel beam and the concrete slab at various locations along the beam length.

**Table 2** The characteristics of the materials used in specimens

Sample	Thickness or diameter (mm)	Fy (MPa)	Fu (MPa)	Elongation at fracture (%)
CFS shear connector plate	2	161	216	12.5
CFS beam and column	3	244	297	12.2
CFS top and seat angle plate	8	157	221	11.5
Reinforcing bar	10	585	660	5.8

## 2.4 Test setup

The specimens installed in the test frame are shown in Fig. 7. The length of the beam was 1.1 m, but it was supported by supports spanning 1 m from the face of the column on each side, and the length of the column used was 0.6 m. The support rests on a roller bearing, while the hinge supports the other end. The composite joints were reversed, with the concrete slab facing down, and the column was subjected to a vertical load. The specimens were loaded using a hydraulic jack and a load cell on the column with a capacity of 300 kN. The load cell readings and LVDT perusals were registered on the data logger and saved on the computer for more analysis.

## 3 Results and discussion

In this section, the experimental outcomes of the five composite cold-formed steel (CFS) beam-to-column joints are outlined. The analysis entails a depiction of the observed behavior of the specimens throughout the tests, evaluating their effectiveness in aspects such as strength, initial stiffness, and rotation. Furthermore, the section delves into elucidating the failure mode, crack propagation, load-slip response, and strain evolution at the joint. A concise summary of the results is provided in Table 3.

### 3.1 Failure mode and crack pattern

The failure modes of all tested specimens in this study are shown in Figs. 8 and 9. It is noted that the failure of all tested specimens was dominated by the significant rotation of the connection angle, which caused the bending of the column flange at the seat angle level and buckled the column's web in the compression zone without the fracture of the longitudinal reinforcing bar. At a load level of about 50–52 kN, the column flange starts buckling under the connection bolt in the compression zone. With an increase in loading to 65 kN, this buckling has become apparent in addition to the buckling in the column web.

Though the significant rotation of the connection angle was observed, the vertical slip between the connection angles and the column flange was not observed. Also, there was no fracture in the connection bolt except for a slight bend of the bolt that connected the angle with the column flange.

### 3.2 Cracking pattern

The cracks of the tested specimens could be seen around the perimeter of the column region and spread diagonally from

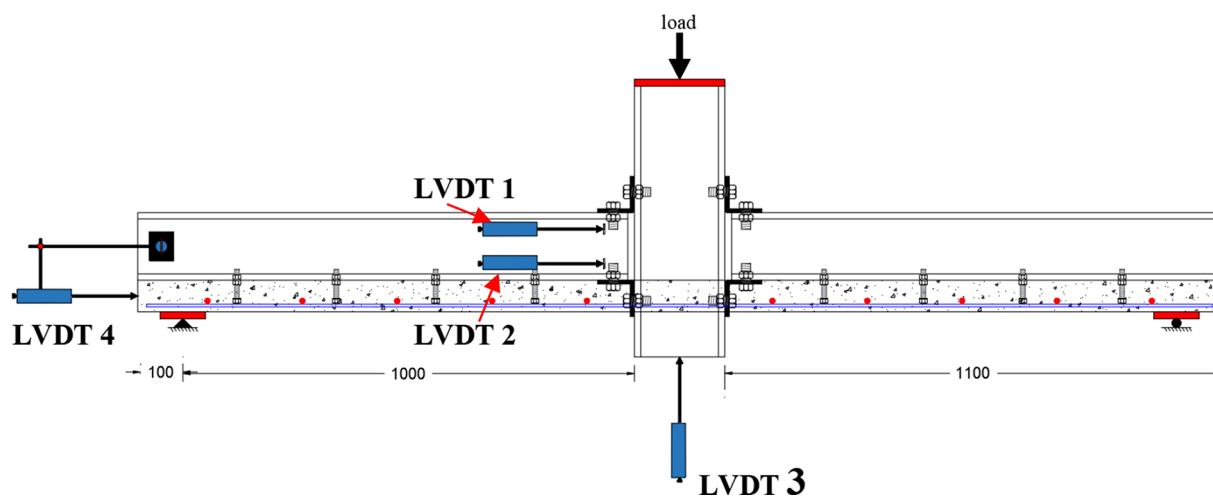


Fig. 6 Location of LVDT used throughout the tests

Fig. 7 Details of Testing Machine Used for composite joint specimens

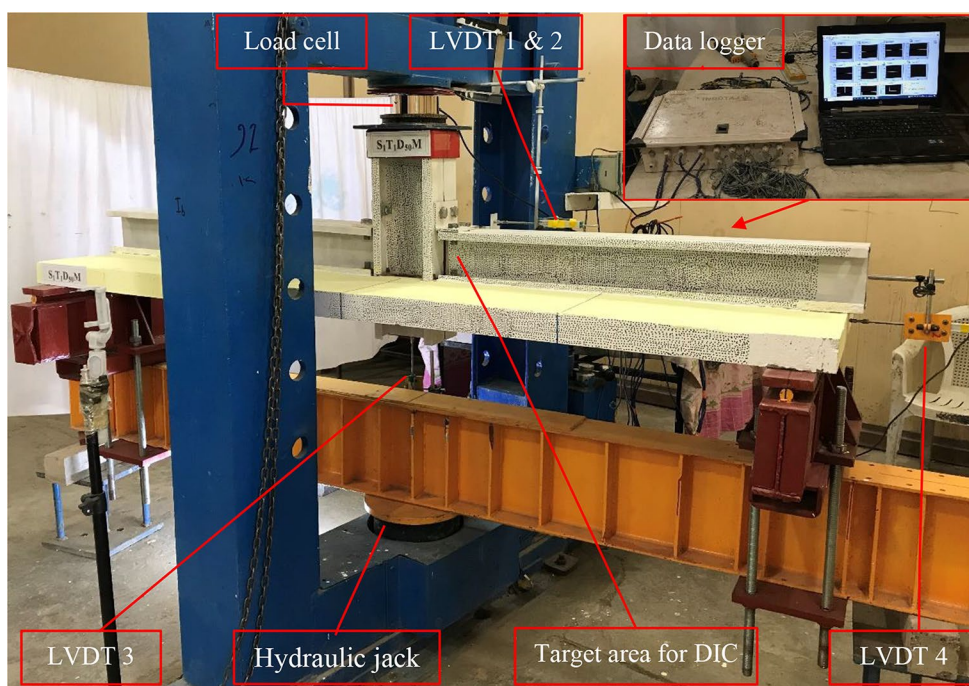


Table 3 Summary of the results of test specimens

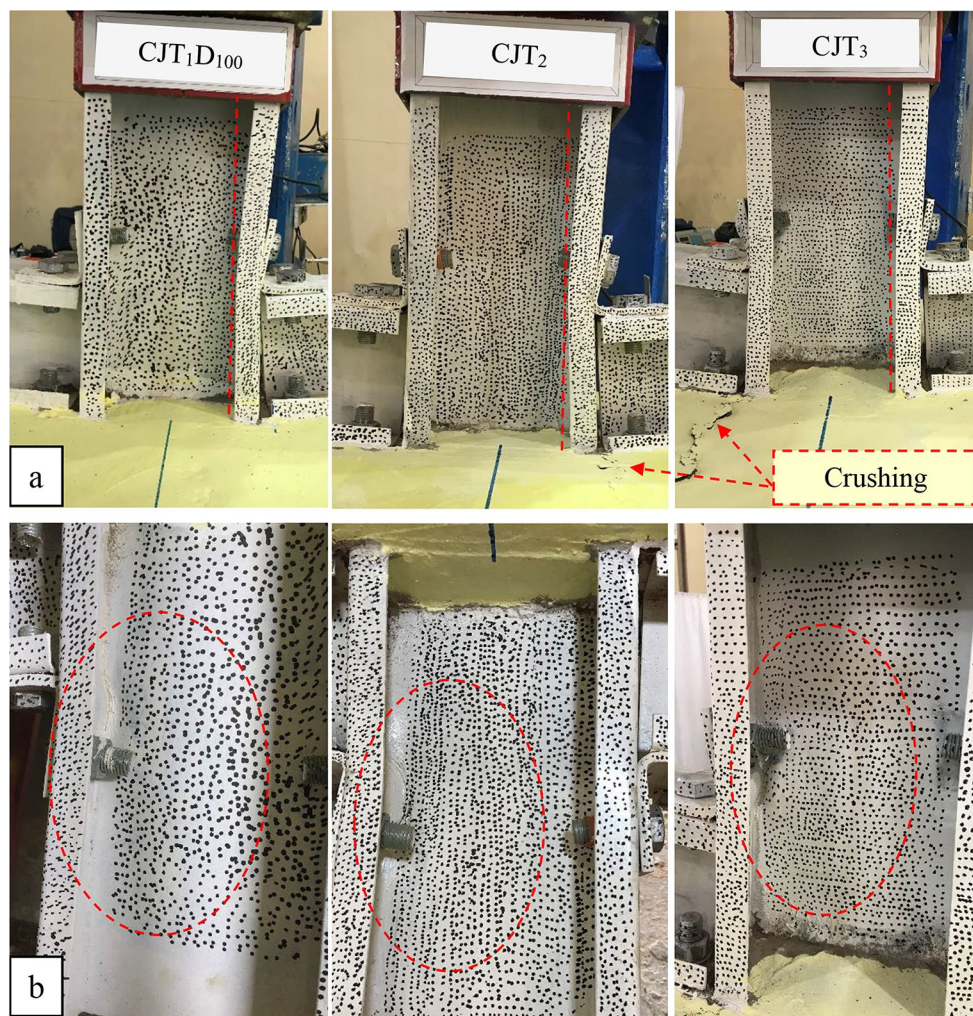
Specimen	Ultimate moment $M_u$ (kN.m)	Rotation $\theta_u$ (mrad)	Slip $\delta_u$ (mm)	Initial stiffness (kN.m/mrad)	Energy absorption (kN.mm)
CJT <sub>1</sub> D <sub>100</sub>	38.28	50.04	0.66	1.54	3731.35
CJT <sub>1</sub> D <sub>50</sub>	37.40	66.75	2.18	1.23	3664.59
CJT <sub>1</sub> D <sub>25</sub>	37.79	89.65	3.40	0.82	3287.84
CJT <sub>2</sub>	43.18	50.16	0.15	2.26	3401.97
CJT <sub>3</sub>	40.48	76.92	1.47	1.91	3045.17

the tips of the column edges to the slab edges (Fig. 10). After that, with increased loading, these cracks formed the dominant transverse cracks across the slab width. The first crack appeared at the column corner at a load of 16.2 kN for specimen CJT<sub>1</sub>D<sub>100</sub> and 10 kN for specimens CJT<sub>2</sub> and CJT<sub>3</sub>. As the load increased, a new transverse crack developed along

the slab width at a distance of 225 mm (the same distance as the first shear connector bolt), 100 mm, and 110 mm from the column face at a load equal to 38, 36, and 36 kN for specimens CJT<sub>1</sub>D<sub>100</sub>, CJT<sub>2</sub>, and CJT<sub>3</sub>, respectively. Then several transverse cracks appeared with increased loading. When the load level reached about 22 kN, the longitudinal



**Fig. 8** Failure mode of specimens with a different type of shear connector: **a** Flange column bending and **b** web buckling



crack appeared, whose extension was parallel to the shear connector from the support to the midspan of the beam. The crushing crack was also observed in specimens CJT<sub>2</sub> and CJT<sub>3</sub> on the concrete's surface near the beam's flange parallel to the column face at 69 kN after the load dropped.

The first visible crack appeared at the corner of the column at a load of 16 kN for specimens CJT<sub>1</sub>D<sub>50</sub> and CJT<sub>1</sub>D<sub>25</sub>. As the load increased, the first crack spread diagonally from the tips of the column edges to the slab edges. New transverse cracks developed on the slab width at load levels 28 and 22 kN for specimens CJT<sub>1</sub>D<sub>50</sub> and CJT<sub>1</sub>D<sub>25</sub>, respectively, at a distance of 100 mm from the column face. When the load level reached 32 and 27 kN for specimens CJT<sub>1</sub>D<sub>50</sub> and CJT<sub>1</sub>D<sub>25</sub>, the cracks developed at a distance of 230 mm from the column face along the slab width. These cracks widened and branched with increased load, and the punching perimeter crack appeared at load level 43 kN. In contrast, the longitudinal crack appeared when the load level reached about 24 and 40 kN for specimens CJT<sub>1</sub>D<sub>50</sub> and CJT<sub>1</sub>D<sub>25</sub>, respectively, whose extension was parallel to

the shear connector from the support to the midspan of the beam.

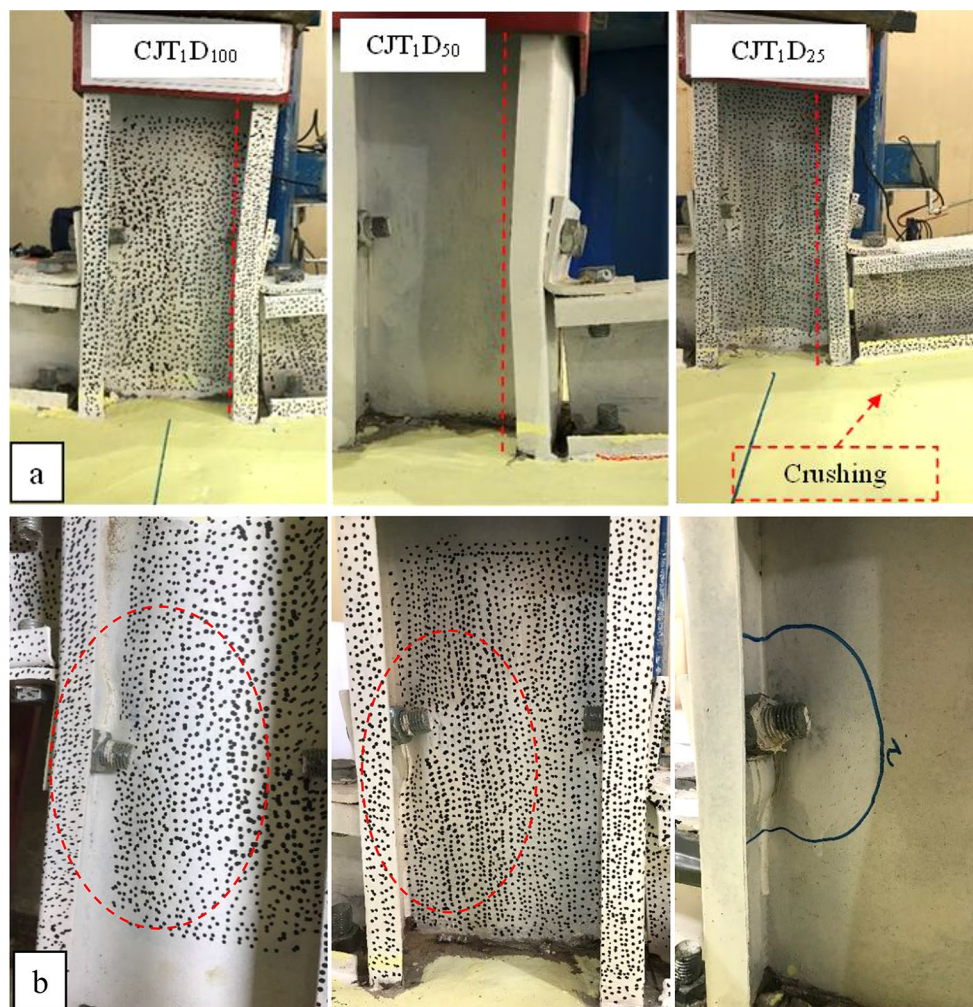
Furthermore, the separation crack between the CFS beam and concrete slab appeared clearly at the support side at load levels of 23 and 14 kN in specimens CJT<sub>1</sub>D<sub>50</sub> and CJT<sub>1</sub>D<sub>25</sub> with a partial shear connection, respectively, compared to specimens CJT<sub>1</sub>D<sub>100</sub> with a full shear connection, which has a slight splitting at higher loads. As the load increased, this separation crack extended until it reached the face of the column and crushed the concrete at the column face after the load reached the ultimate.

### 3.3 Moment-rotation curve

The moment-rotation curves for specimens CJT<sub>1</sub>D<sub>100</sub>, CJT<sub>2</sub>, and CJT<sub>3</sub> are shown in Fig. 11. All these specimens possessed high ductile properties where the rotation capacity exceeded 30 mrad. Hence, all these specimens classify as semi-rigid joints according to Eurocode 4 (EC4) [21], which specifies bolted joints' classification by rotational capacity. Specimens CJT<sub>1</sub>D<sub>100</sub> and CJT<sub>2</sub> have the same rotational



**Fig. 9** Failure mode of specimens with different degrees of shear connector: **a** Flange column bending and **b** web buckling



capacity with a slight difference in the ultimate moment. In contrast, specimen  $CJT_3$  has a higher rotational capacity of 54% compared with the other specimens. The increase in rotation capacity for specimen  $CJT_3$  is due to an increased slip between the concrete slab and the CFS beam, which, by reducing the level of the shear connector, leads to an increase in slippage and, thus, an increase in the amplitude of joint rotation. The values of moment and rotation are also listed in Table 3.

On the other hand, Fig. 12 shows the moment-rotation curves for specimens  $CJT_1D_{100}$ ,  $CJT_1D_{50}$ , and  $CJT_1D_{25}$ . All these specimens possessed high ductile properties where the rotation capacity exceeded 30 mrad. As the bolted shear connector was reduced in the composite joints, there was no discernible difference in strength, but this was accompanied by increased rotation capacity. This corresponds to [7] reaching for a head stud connector with hot-rolled steel. The rotational capacity of specimens  $CJT_1D_{50}$  and  $CJT_1D_{25}$  increased by 33.4% and 79.16%, respectively, compared with specimen  $CJT_1D_{100}$ , which has a full degree of shear connection. This indicated that the partial shear connector is

a beneficial in ductility but caused a reduction in the initial rotational stiffness.

### 3.4 Initial stiffness

In terms of stiffness, the initial stiffness is between  $0.5EI_b/L_b$  and  $25EI_b/L_b$ , indicating that the corresponding joint is a semi-rigid connection according to Eurocode 3 (EC3) [22]. The stiffness value for specimens with different shear connector types is shown in Fig. 13, in which specimen  $CJT_2$  showed higher initial stiffness than other specimens due to using a CFS angle plate as a shear connector, which increases flexural resistance and thus increases stiffness.

Furthermore, the initial rotational stiffness is decreased by reducing the level of the shear connector. The initial rotational stiffness decreased by 20% and 47% for specimens  $CJT_1D_{50}$  and  $CJT_1D_{25}$ , respectively, compared to specimen  $CJT_1D_{100}$ , as shown in Fig. 14. This is due to higher slip displacements for specimens with a lower degree of shear connection; which causes higher rotational capacity and thus reduces stiffness.

**Fig. 10** Crack pattern of the tested specimens: **a** CJT<sub>1</sub>D<sub>100</sub>, **b** CJT2 and **c** CJT3

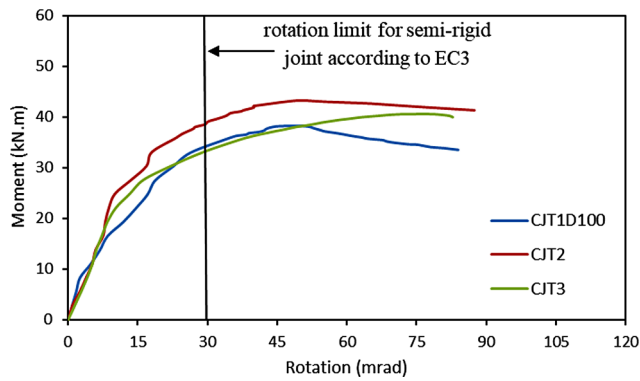
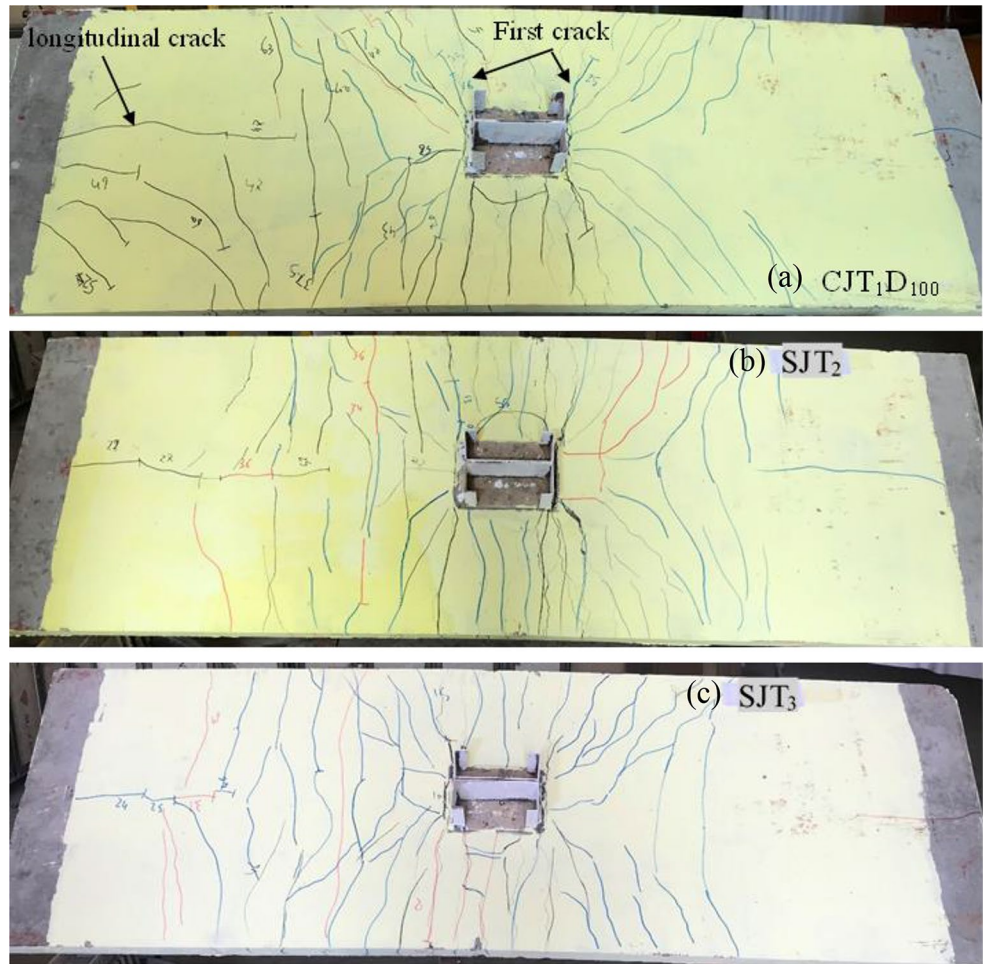


**Fig. 11** The moment-rotation curve of specimens with different shear connector types

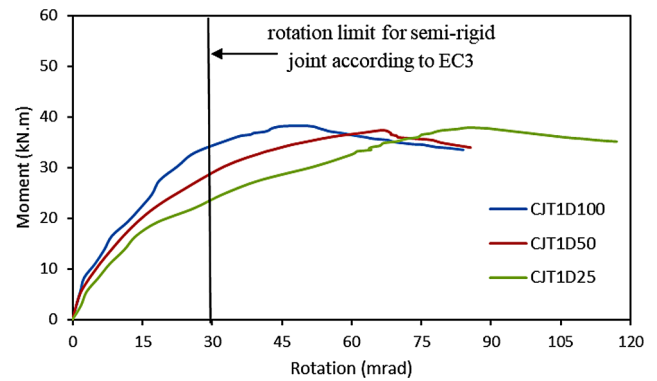


**Fig. 12** The moment-rotation curve of specimens with different shear connector degrees

### 3.5 Load-slip curves

The slip values at the ultimate load for all tested specimens are listed in Table 3. The shear connector did not fail in any of the tests. As expected, specimen CJT<sub>1</sub>D<sub>25</sub> had the greatest slip because it has the slightest degree of shear connection. The load-slip behavior of the specimens in each group is shown in Figs. 15 and 16. As demonstrated by the

CJT<sub>1</sub>D<sub>50</sub> and CJT<sub>1</sub>D<sub>25</sub> test results, the slip value increased as the degree of shear connection decreased because of partial interactive behavior. While in the other specimens, the slip value was small due to the availability of full interactive behavior. In addition, providing a high ratio of reinforcement cause a limited extension of the reinforcement; thus, slippage between the steel beam and concrete slab is reduced.

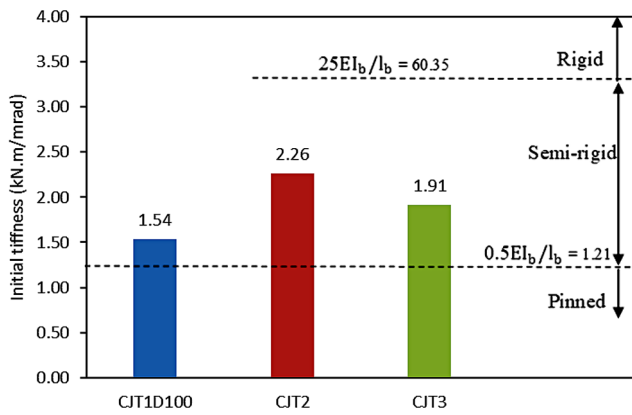


Fig. 13 Effect of shear connection type on the initial stiffness response

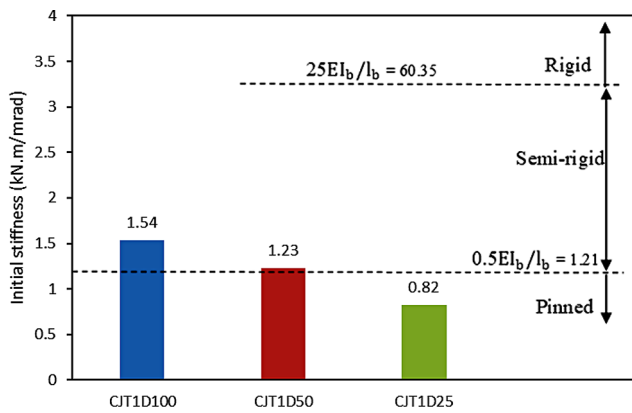


Fig. 14 effect of bolted shear connection degree on the initial stiffness response

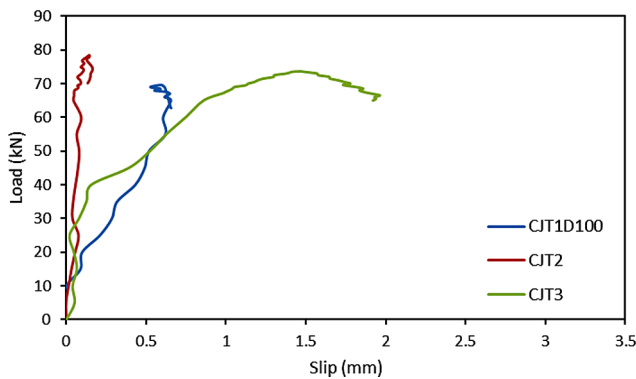


Fig. 15 Load-slip response for specimens with different shear connector types

Figure 17 shows the slip response along the beam span at various load levels for all tested specimens. Slip behavior was found to be symmetrical from the beginning of loading and increased as the load approached the maximum load. The highest slip was also observed at the beam ends, near the supports.

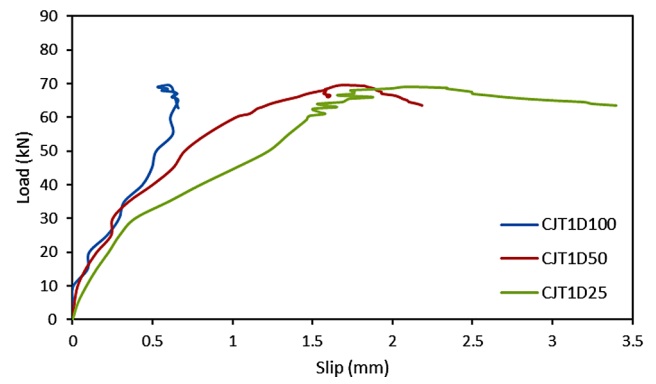


Fig. 16 Load-slip response for specimens with different degrees of the bolted shear connector

### 3.6 Composite CFS beam strains

The strain profile through the depth of the composite CFS beam at the column face is measured using the DIC technique at ultimate load, as shown in Figs. 18 and 19. It demonstrates that the steel beams in partial shear connection joints CJT<sub>1</sub>D<sub>50</sub> and CJT<sub>1</sub>D<sub>25</sub> were more strained than CJT<sub>1</sub>D<sub>100</sub>. It is also worth noting the more pronounced change in the neutral axis position for specimens CJT<sub>2</sub> and CJT<sub>3</sub> compared to specimen CJT<sub>1</sub>D<sub>100</sub>, which can be attributed to the reinforcement and steel beam’s more extensive inelastic yielding in specimen CJT<sub>1</sub>D<sub>100</sub>. While the specimen CJT<sub>2</sub>, which has a CFS plate angle shear connector, reduces the strains generated in the concrete slab and CFS beam. Also, from Figs. 17 and 18, and 19, it was noticed that when the slippage between the concrete slab and the steel beam increases, the strain at the column face decreases through the slab depth. Specimen SJT<sub>2</sub>, which has the least slippage, noticed that the strain in Fig. 18 is very small compared to the other specimens.

## 4 Conclusion

Five specimens with cruciform subassemblies of composite cold-formed steel beam-to-column joints connected by top and seat angles were prepared to investigate the structural performance, including the initial stiffness, moment and rotational capacities, and slip response. For this purpose, two variables were considered: the types of shear connection (bolted shear connector with single embedded nut, CFS plate angle, and CFS plate corrugated) and the degree of bolted shear connector (16-bolt, eight bolt, and four-bolt). The main findings are listed as follows:

1. The top and seat angle connections between the semi-rigid CFS beam-to-column joints exhibit high ductility where the rotational capacity corresponding to the



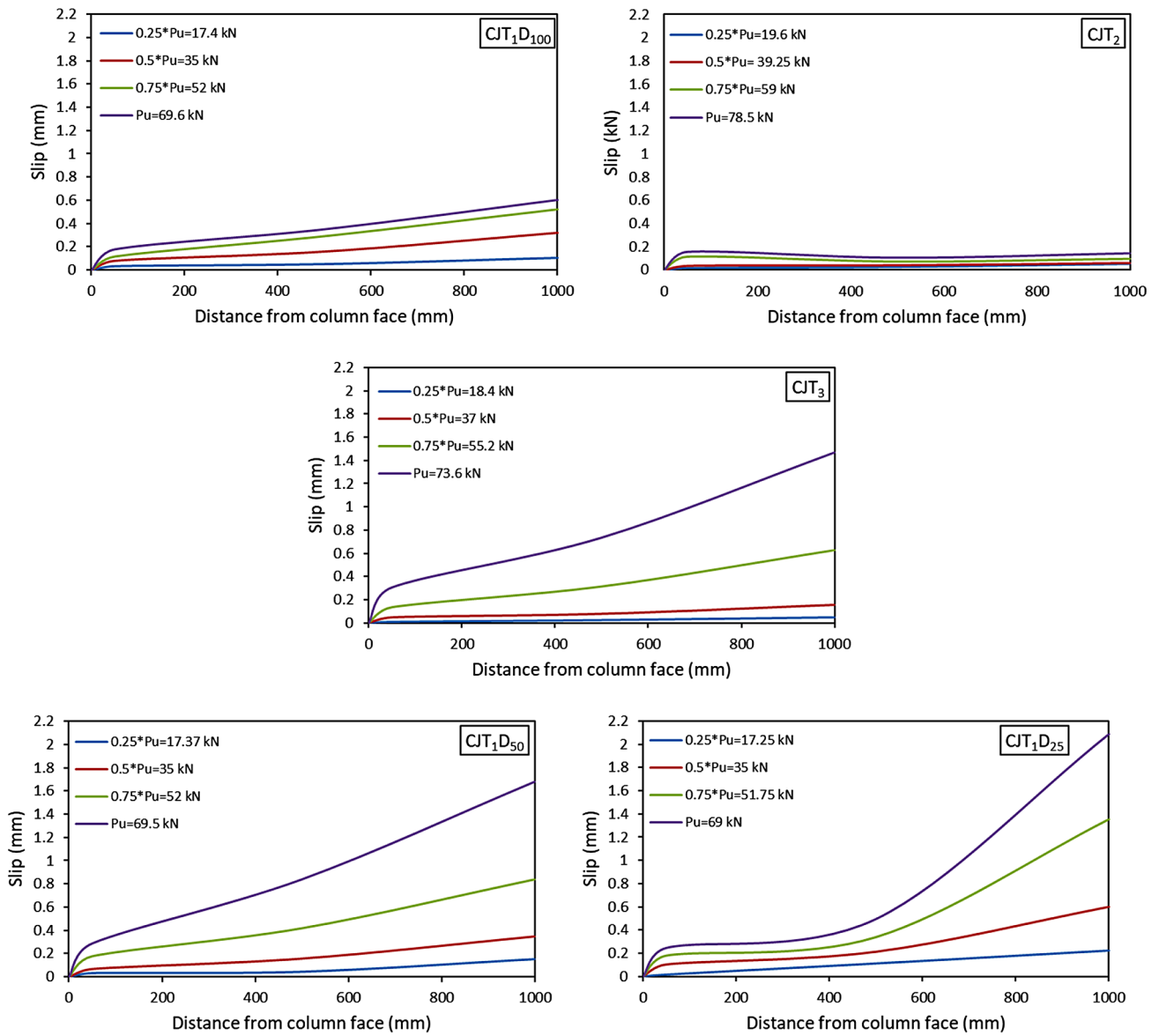


Fig. 17 The slip response along beam span for all specimens

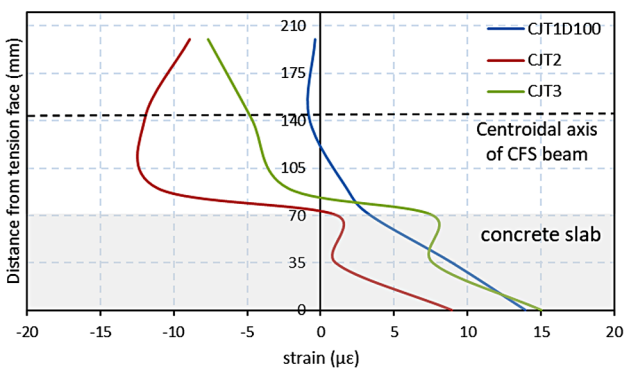


Fig. 18 CJT<sub>1</sub>D<sub>100</sub>, CJT<sub>2</sub> and CJT<sub>3</sub> strain distribution at various cross-sections as measured from the column face

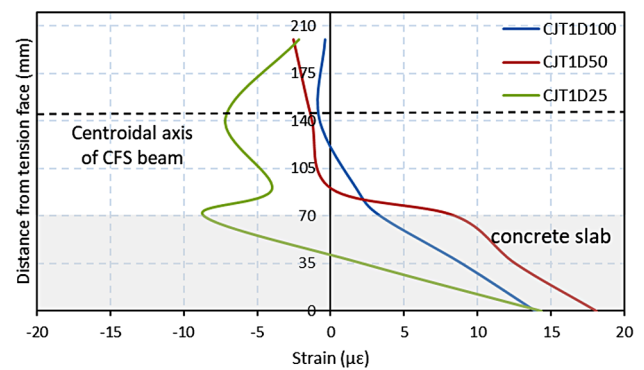


Fig. 19 CJT<sub>1</sub>D<sub>100</sub>, CJT<sub>1</sub>D<sub>50</sub> and CJT<sub>1</sub>D<sub>25</sub> strain distribution at various cross-sections as measured from the column face

ultimate moment exceeds 30 mrad. As a result, they are adequate for plastic analysis and seismic design.

2. The CFS angle plate shear connector increases the moment capacity and initial stiffness by about 12% and 47%, respectively, compared with specimen CJT<sub>1</sub>D<sub>100</sub>, which has a fully bolted shear connector while maintaining the same rotational capacity.
3. Compared to specimen CJT<sub>1</sub>D<sub>100</sub>, which has a full degree of shear connection, the rotational capacities of specimens CJT<sub>1</sub>D<sub>50</sub> and CJT<sub>1</sub>D<sub>25</sub> with partial shear connectors increased by 33.4% and 79.16%, respectively. This demonstrated that the partial shear connector improved ductility while decreasing initial rotational stiffness.
4. When the shear connector ratio was reduced, the initial rotational stiffness decreased by 20% and 47%, respectively, for specimens CJT<sub>1</sub>D<sub>50</sub> and CJT<sub>1</sub>D<sub>25</sub>, compared to specimen CJT<sub>1</sub>D<sub>100</sub>, due to higher slip displacements for specimens with a lower degree of shear connection.
5. Compared to fully shear connected, using a partially bolted shear connector up to 50% of fully shear connected produced acceptable results and was within the recommended limits for semi-rigid joints according to the European Code.
6. Based on the observations, the failure patterns are dominated by the yielding of connection angles since large deflections and rotations occur on the top and seat CFS angles. So, it is recommended to use an angle of 10 mm thickness to obtain higher strength with rotational capacity, which also gives a semi-rigid behavior (ductility behavior).

**Acknowledgements** The specimens test was performed in the structural laboratory of the Civil Engineering Department at Babylon University. So, the authors express their gratitude and sincere appreciation for this establishment. We are grateful to all the friends who helped and supported completing this work.

**Author contributions** Mustafa S. S: wrote the main manuscript text and prepared all figures and tables in the manuscript. H. H. M reviewed and modified the manuscript. All authors reviewed the manuscript.

**Funding** No funding was received to assist with the preparation of this manuscript.

**Data availability** All data available in manuscript text.

## Declarations

**Competing interests** The authors declare no competing interests.

## References

1. Salah MS, Muteb HH, Hamad MA (2023) The structural behavior of composite cold-formed steel beam-to-column joints with different connection shapes. *J Building Pathol Rehabilitation* 8(1):50. <https://doi.org/10.1007/s41024-023-00304-3>
2. Yu WK, Chung KF, Wong MF (2005) Analysis of bolted moment connections in cold-formed steel beam-column sub-frames. *J Constr Steel Res* 61(9):1332–1352. <https://doi.org/10.1016/j.jcsr.2005.03.001>
3. Li JT, Li GQ, Lou GB, Chen LZ (2012) Experimental investigation on flush end-plate bolted composite connection in fire. *J Constr Steel Res* 76:121–132. <https://doi.org/10.1016/j.jcsr.2012.03.022>
4. Song TY, Tao Z, Razzazzadeh A, Han LH, Zhou K (2017) Fire performance of blind bolted composite beam to column joints. *J Constr Steel Res* 132:29–42. <https://doi.org/10.1016/j.jcsr.2017.01.011>
5. Hamad MA, Muteb HH (2023) Influence of loading direction on X-HVB shear connectors in partially composite steel-concrete beams exposed to fire. *Innovative Infrastructure Solutions* 8(9):234. <https://doi.org/10.1007/s41062-023-01206-6>
6. Fu F, Lam D (2006) Experimental study on semi-rigid composite joints with steel beams and precast hollowcore slabs. *J Constr Steel Res* 62(8):771–782. <https://doi.org/10.1016/j.jcsr.2005.11.013>
7. Loh HY, Uy B, Bradford MA (2006) The effects of partial shear connection in composite flush end plate joints Part I—experimental study. *J Constr Steel Res* 62(4):378–390. <https://doi.org/10.1016/j.jcsr.2005.07.012>
8. Ataei A, Bradford MA, Valipour HR (2015) Experimental study of flush end plate beam-to-CFST column composite joints with deconstructable bolted shear connectors. *Eng Struct* 99:616–630. <https://doi.org/10.1016/j.engstruct.2015.05.012>
9. Salih MNA, Tahir MM, Mohammad S, Ahmad Y (2019) Behavior of Boxed Cold-Formed Steel as Composite Beam with Rebar as Shear Connector. In: Rodrigues H, Elnashai A (eds) *Advances and challenges in Structural Engineering*. GeoMEast 2018. Sustainable civil infrastructures. Springer, Cham. [https://doi.org/10.1007/978-3-030-01932-7\\_25](https://doi.org/10.1007/978-3-030-01932-7_25)
10. Lakkavalli BS, Liu Y (2006) Experimental study of composite cold-formed steel C-section floor joists. *J Constr Steel Res* 62(10):995–1006. <https://doi.org/10.1016/j.jcsr.2006.02.003>
11. Irwan JM, Hanizah AH, Azmi I (2009) Test of shear transfer enhancement in symmetric cold-formed steel-concrete composite beams. *J Constr Steel Res* 65(12):2087–2098. <https://doi.org/10.1016/j.jcsr.2009.07.008>
12. Lawan MM, Tahir MM, Osman MH (2015) Composite construction of cold-formed steel (CFS) section with high strength bolted shear connector. *Jurnal Teknologi*, 77(16)
13. Lawan MM, Tahir MM, Hosseinpour E (2016) Feasibility of using bolted shear connector with cold-formed steel in composite construction. *Jurnal Teknologi* 78:6–12
14. Hamad MA, Muteb HH, Salah MS (2023) Investigating the behavior of composite steel-concrete beams with X-HVB shear connectors exposed to various fire temperature levels. *J Building Pathol Rehabilitation* 8(2):1–16. <https://doi.org/10.1007/s41024-023-00340-z>
15. Bezerra LM, Cavalcante OO, Chater L, Bonilla J (2018) V-shaped shear connector for composite steel-concrete beam. *J Constr Steel Res* 150:162–174. <https://doi.org/10.1016/j.jcsr.2018.07.016>
16. Salah MS, Muteb HH (2023) The effect of cross section type on the performance of different sized bolted shear connectors for composite cold-formed steel beams. *J Build Rehabil* 8:5. <https://doi.org/10.1007/s41024-022-00252-4>

17. Jiang H, Fang H, Liu J, Fang Z, Zhang J (2021), October Experimental investigation on shear performance of transverse angle shear connectors. In *Structures* (Vol. 33, pp. 2050–2060). Elsevier. <https://doi.org/10.1016/j.istruc.2021.05.071>
18. Nouri K, Sulong NR, Ibrahim Z, Shariati M (2021) Behaviour of novel stiffened angle shear connectors at ambient and elevated temperatures. *Adv Steel Constr* 17(1):28–38
19. Bamaga SO, Tahir MM, Tan CS, Shek PN, Aghlara R (2019) Push-out tests on three innovative shear connectors for composite cold-formed steel concrete beams. *Constr Build Mater* 223:288–298. <https://doi.org/10.1016/j.conbuildmat.2019.06.223>
20. ASTM A (2005) 370-05, Standard Test Method and Definition for Mechanical Testing of Steel Products, Annual Book of ASTM Standard, Vol. 01.01. ASTM, Philadelphia, PA
21. EN1994-1-1(2004), Eurocode 4: design of Composite Steel and concrete structures. Part 1–1: General rules and rules for buildings. Brussels, Belgium: European Committee for Standardization
22. Standard B (2006) Eurocode 3—Design of steel structures—. BS EN 1993-1, 1, 2005

**Publisher's Note** Springer Nature remains neutral with regard to jurisdictional claims in published maps and institutional affiliations.

Springer Nature or its licensor (e.g. a society or other partner) holds exclusive rights to this article under a publishing agreement with the author(s) or other rightsholder(s); author self-archiving of the accepted manuscript version of this article is solely governed by the terms of such publishing agreement and applicable law.